Article

The Chart Diagnostic System Improves the Diagnostic Accuracy of Cervical Lymph Node Metastasis in Oral Squamous Cell Carcinoma

Ayako Nomura [1], Takayuki Ishida [1,*], Hiroshi Hijioka [2], Takuya Yoshimura [1], Hajime Suzuki [1], Eturo Nozoe [1] and Norifumi Nakamura [1]

1 Department of Oral and Maxillofacial Surgery, Graduate School of Medical and Dental Sciences, Kagoshima University, Kagoshima 890-8544, Japan
2 Department of Maxillofacial Diagnostic and Surgical Sciences, Graduate School of Medical and Dental Sciences, Kagoshima University, Kagoshima 890-8544, Japan
* Correspondence: taka-isi@dent.kagoshima-u.ac.jp; Tel.: +81-99-275-6242

Simple Summary: The presence of cervical lymph node metastasis is the most important prognostic factor in oral squamous cell carcinoma (OSCC). Therefore, the detection of metastatic lymph nodes before treatment is most important to improve patient prognosis. The purpose of this study was to combine imaging findings of cervical lymph nodes and histopathological factors of biopsy specimens associated with cervical lymph node metastasis in OSCC. Our results suggest that cervical lymph node metastasis is related to the internal echo of ultrasonography (US), rim enhancement of enhanced Computed Tomography (CT), vascular invasion, and Yamamoto–Kohama (YK) classification of biopsy specimens. We have established new diagnostic criteria combining these factors. This strategy may reduce false negative diagnoses of cervical lymph node metastasis.

Abstract: Purpose: To establish a diagnosis method based on imaging findings and histopathological factors associated with cervical lymph node metastasis. Methods: A total of 1587 cervical lymph nodes that were detected using imaging tools in 73 OSCC patients who underwent surgical treatment were enrolled to evaluate the association between imaging findings (long diameter, short diameter, long–short ratio, US findings (hilum and internal echo), contrast effect with enhanced CT, standardized uptake value (SUV) max and SUV average with ^{18}F FDG-Positron Emission Tomography (PET)) and metastatic cervical lymph nodes. In 57 OSCC patients, biopsy specimens were evaluated for histopathologic factors (budding score, lymphatic invasion, vascular invasion, nerve invasion, and YK classification) and the presence of cervical lymph node metastases. Cervical lymph node metastasis was determined based on histopathological examination of the lymph nodes of patients with no metastasis observed 3 years after primary surgery. Results: In total, 22 of the 73 patients had cervical lymph node metastasis pathologically. In the comparison of the presence of metastatic lymph nodes, univariate analysis showed significant differences in cervical lymph node long and short diameter, long/short ratio, internal echo, rim enhancement, SUV max, SUV average, budding score, and vascular invasion. Multivariable analysis showed significant differences in internal echo, rim enhancement, SUV max, and budding score. Conclusions: We propose a chart diagnostic system that combines imaging and histopathological findings to improve the diagnosis of cervical lymph node metastasis.

Keywords: oral squamous cell carcinoma; metastasis; diagnosis

1. Introduction

The presence of cervical lymph node metastasis is the greatest poor prognostic factor for oral squamous cell carcinoma (OSCC) [1,2]. In particular, late cervical lymph node metastasis, which does not show metastasis during initial treatment and becomes apparent

during follow-up, often has extranodal invasion and poor prognosis. Pretreatment evaluation of cervical lymph node metastasis is important in the treatment planning and prognosis of OSCC patients. Preoperative cervical lymph node status is usually assessed using clinical examination, including palpation, Ultrasonography (US), Computed Tomography (CT), Magnetic Resonance Imaging (MRI), and ^{18}F FDG-Positron Emission Tomography (PET). Despite the development of diagnostic imaging techniques, the incidence of secondary metastasis has been estimated at 6–50% [2–5]. Treatment plans and strategies for OSCC patients who are clinically diagnosed with negative cervical lymph node metastasis (cN0) remain controversial. To improve the accuracy of OSCC cervical lymph node metastasis diagnosis, our department has established chart-based diagnostic criteria using CT, US, and PET and has revised the evaluation over a period of time [6]. As a result, the secondary metastasis rate was reduced, and the disease-specific survival rate was also improved. However, there is still a problem with the number of false negatives and false positives because micro lymph node metastasis did not appear as a clear sign using imaging. Therefore, further factors are needed to improve diagnostic accuracy. The presence of vascular or lymphatic invasion has been reported in the past as a predictor of lymph node metastasis other than imaging [7], and recently, it has been reported that the budding score is also a useful predictor of metastasis [8–10]. However, most of these are examined with resection specimens, and there are few reports on biopsy sections. The purpose of this study was to establish the preoperative diagnostic system by combining imaging findings and histopathological factors obtained from biopsy sections to the image diagnostic criteria used in our department. Then, we examined the evaluation items of the image diagnosis and the histopathological evaluation items again and searched for the factors contributing to cervical lymph node metastasis.

2. Materials and Methods

2.1. Patients

Seventy-three patients with primary OSCC who received surgical treatment between March 2010 and October 2015 in the Department of Oral and Maxillofacial Surgery at Kagoshima University Hospital were included in this study. All patients were evaluated using contrast-enhanced CT, US, and FDG-PET/CT before initial treatment. Ultimately, the study involved 73 patients. They were 44 men and 29 women, with an average age at diagnosis of 66.1 ± 12.5 years and a range of 29–91 years, who could be evaluated for cervical lymph node status. Both the clinical and pathological stagings were performed according to the Union for International Cancer Control TNM classification (2010, 7th edition). Neck dissection was planned by our department based on clinical and imaging findings. With tumors larger than 3 cm in size (late T2), patients received preoperative chemoradiotherapy consisting of S-1, and the prescribed dose was 30 Gy in 15 fractions, and radical surgery was performed within 1 month after preoperative treatment. All cN(+) and cN0 patients who required reconstructive surgery underwent neck dissection simultaneously with primary tumor resection. If even one node was diagnosed with metastasis before treatment, a radical neck dissection with ipsilateral levels I–V was performed. The sternocleidomastoid muscle was always sacrificed, and the accessory nerves and internal jugular vein were preserved unless there were metastatic lymph node attachments. cN0 patients who needed reconstructive surgery underwent a supraomohyoid neck dissection. After surgery, all patients were clinically examined by surgeons once or twice a month in year 1, once a month in year 2, and every 3–6 months in years 3–5. Enhanced CT and US were performed 1, 3, 6, 12, 18, and 24 months after surgery and once a year for the next 3 years. If cervical node metastasis was detected during observation, then neck dissection and a histopathological examination were performed immediately.

2.2. *Image Analysis*

2.2.1. Protocol for Contrast-Enhanced CT and US

Using the contrast-enhanced CT or US images, each cervical lymph node was evaluated for the long diameter, short diameter, and long and short ratio. The existence of a hilum and internal echo were investigated using US. The enhanced pattern of lymph nodes was evaluated using contrast-enhanced CT.

2.2.2. Protocol for ^{18}F FDG-PET/CT

Overall, ^{18}F FDG-PET/CT has been recognized as a useful tool to identify metastatic lymph nodes. In this study, images were obtained using Discovery PET/CT 600 Motion and Discovery PET/CT 610 Motion (GE healthcare, Chicago, IL, USA). After fasting for 6 h before FDG-PET/CT scanning, patients were administered ^{18}F FDG at a concentration of 3.7 MBq/kg body weight. Whole body scanning was performed 1 h after ^{18}F FDG dosing, and local images were obtained 2 h later. FDG uptake in lesions was evaluated using the standardized uptake value (SUV) max and SUV average calculated with the maximum area of each lymph node for quantitative analysis at 2 h later scanned images.

2.3. *Diagnosis of Clinical Nodal Status*

Comprehensively, the node status was determined using various combinations of some modalities, CT, US, and FDG-PET/CT. The diagnostic criteria of metastasis were shown in our previous study [6]. Cervical lymph nodes were considered positive if at least CT or US was positive. If all results were suspect or negative, the final diagnosis was based on FDG-PET. The SUV max of the lymph node was considered positive if its SUV max was larger than 3.2.

2.4. *Pathological Examination*

The biopsy specimens of 57 patients could be evaluated. Biopsies were performed by experienced oral oncologists and included the border between the lesion and normal tissue. These biopsy specimens were examined for tumor budding score, lymphovascular invasion, vascular invasion, perineural invasion, and Yamamoto–Kohama (YK) classification. Lymphatic invasion, vascular invasion, perineural invasion, and YK classification were diagnosed by oral pathologists. Tumor budding was defined according to the ITBCC scoring system as a single cell or a cell cluster comprising less than 5 cancer cells at the invasive front. All hematoxylin and eosin-stained slides were reviewed three times separately by two oral surgeons who were blinded to the clinical data independently of blinded patient information, and the mean value was adopted. After the selection of one field by which budding was the most intensive, the number of buds was counted using a 20 × 10 objective lens.

2.5. *Definite Diagnosis of Cervical Lymph Nodal Status*

In patients who underwent neck dissection, we considered their pathological N status to be their "true N status = pN(+)". In patients who did not undergo neck dissection, at least 36 months of follow-up data were examined for the presence of nodal metastases = pN(−).

2.6. *Statistical Analysis*

All statistical analyses were performed using JMP version 9.0.2 (SAS Institute Inc., Cary, NC, USA) to determine the significance between the pN(+) and pN(−) lymph node groups. The distribution of clinical and pathological factors in the pN(+) and pN(−) lymph node groups was tested using the χ^2 test. ROC analysis was used to evaluate cut-off values for SUV max, SUV average, and the budding score. Multivariable logistic regression was used to predict lymph node metastasis based on various clinical and pathological factors. The results of the univariate and multivariable analyses were presented as the odds ratio (OR) and 95% confidence interval (CI). The factors using multivariable analyses were enrolled using the forward stepwise selection method ($p \leq 0.2$). To evaluated sample size

adequacy, the power was calculated with effect size = 0.8 and α = 0.05 by a post hoc test using G*Power 3.1 (free software).

3. Results

In this study, we included 1584 cervical lymph nodes of 72 OSCC patients to evaluate the association between imaging findings and metastasis and evaluated another 57 patients with biopsy pathology findings. To evaluate the validity of this cohort study, we used a post hoc test to assess the power (Supplementary Table S1).

The 72 OSCC patients were clinically classified into a 38 cN($-$) group and a 35 cN(+) group before surgery. Twenty-two patients had cervical lymph node metastasis pathologically. There were no significant differences in age, sex, cT classification, or primary location among them (Table 1).

Table 1. Patient population.

	pN(+) Group	pN($-$) Group	*p* Value
Number	22	51	
age	64.7 $\pm$ 14.0	67.1 $\pm$ 12.1	0.462
sex			
male	14	30	0.699
female	8	21	
cT clssification			
T1	3	10	0.629
T2	14	27	
T3	4	8	
T4	1	6	
Primary tumor			
Tongue	11	22	0.419
Floor of mouth	2	6	
Mandibular	32	12	
Maxilla	4	8	
Buccal mucosa	2	3	
cN0	7	31	0.018 *
cN1/2	15	20	
late metastasis	5	0	-

* *p* < 0.05.

Twenty-nine cN0 patients did not undergo neck dissection as their primary surgical treatment and adopted the wait-and-watch policy. Five (17.2%) of them developed cervical node metastasis without recurrence at the primary local site during the follow-up period, and rescue surgery was performed as soon as metastasis was detected.

A total of 1587 cervical lymph nodes (average 21.7 per patient, range 12–37) were analyzed using image examinations. Of those lymph nodes, 33 nodes showed metastasis pathologically, and 1554 nodes were either histologically non-metastatic or did not show metastasis on follow-up. The imaging findings of each lymph node were compared between pN(+) nodes and pN($-$) nodes (Table 2). The values of the imaging features were not normally distributed. There were significant differences in the lymph node long diameter, short diameter, long/short ratio, internal echo, CT contrast effect, SUV max, and SUV average (Figure 1). The long diameter and short diameter of the metastatic lymph nodes were significantly longer than those of the lymph nodes without metastasis. The long/short ratio of the metastatic lymph nodes was significantly shorter than that of the lymph nodes without metastasis. The ROC curve cut-off values, AUC, sensitivity, and specificity of the long diameter, short diameter, and long/short ratio were 9.14 vs. 5.20 vs. 1.55, 0.761 vs. 0.826 vs. 0.626, 66.7% vs. 66.7% vs. 48.5%, and 41.4% vs. 43.1% vs. 65.8%, respectively (data not shown).

Table 2. Classification of imaging factors of lymph nodes and logistic regression analysis for imaging factors predicting lymph node metastasis.

Imaging Feature	pN(+) LNs	pN(−) LNs	χ^2 Test *p* Value	Result of Logistic Regression Analysis					
				Univariate Analysis			Multivariable Analysis		
	n = 33	*n* = 1554		OR	95% Cl	*p* Value	OR	95% Cl	*p* Value
Long diameter	11.1 (7.1–17.4)	6.0 (4.6–8.2)	<0.001 **	1.23	1.16–1.31	<0.001 **	-	-	-
Short diameter	4.6 (3.6–5.9)	2.7 (2.0–3.6)	<0.001 **	1.98	1.67–2.36	<0.001 **	-	-	-
Long/Short ratio	1.9 (1.3–2.9)	2.2 (1.8–2.9)	0.042 *	0.60	0.36–0.94	0.038 *	-	-	-
US observation Hilum Clear/unclear disappearance	21/6 6	687/569 298	0.886	0.94	0.89–2.14	0.885	-	-	-
Internal echo None/unclear Appearance	14/4 17	1452/87 15	<0.001 **	109.0	47.1–260.9	<0.001 **	16.37	4.00–57.78	<0.001 **
CT contrast effect None/heterogeneity Rim enhancement	14/5 14	1506/43 5	<0.001 **	228.3	79.1–767.5	<0.001 **	5.58	1.08–31.64	0.045 *
SUV max	3.5 (2.3–5.4)	1.0 (1.0–1.0)	<0.001 **	2.51	2.07–3.10	<0.001 **	2.11	1.66–2.68	<0.001 **
SUV average	2.6 (1.9–3.4)	1.0 (1.0–1.0)	<0.001 **	4.51	3.26–6.45	<0.001 **	-	-	-

Long diameter, Short diameter, Long/Short ratio, SUV max, and SUV average indicate median and interquartile range. LN: lymph node, OR: odds ratio, Cl: confidence interval. * $p < 0.05$, ** $p < 0.01$.
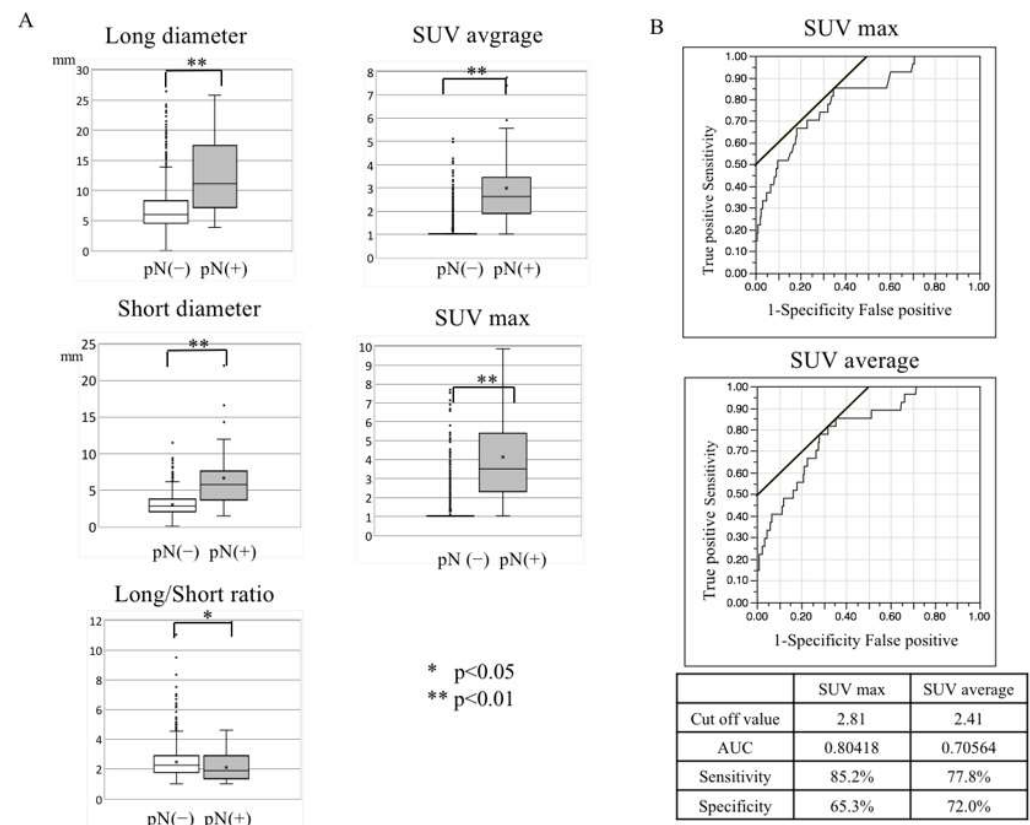

Figure 1. (**A**): Distribution of imaging factors in metastatic lymph nodes and non-metastatic lymph nodes. The central line is the median. The central mark "×" is average. The box is the 25–75% confidence interval. The vertical line is the 95% confidence interval. The dots are outliers. (**B**): ROC curve and cut-off value of SUV max and SUV average.

Most negative lymph nodes showed an FDG concentration equal to that of normal tissue, and their SUV max and SUV average were distributed at 1.0; therefore, the SUV max and SUV average of the metastatic lymph nodes were significantly higher than those of the negative lymph nodes.

The ROC curve cutoff values, AUC, sensitivity, and specificity of the SUV max and SUV average were 2.81 vs. 2.41, 0.804 vs. 0.706, 85.2% vs. 77.8%, and 65.3% vs. 72.0%,

respectively. Logistic regression was applied to identify predictive lymph node metastasis in the imaging factor. Based on the univariate analysis of the imaging factors, the long diameter, short diameter, long/short ratio, internal echo, CT contrast effect, SUV max, and SUV average were significantly associated with lymph node metastasis. As a result of the forward stepwise selection method, three factors (internal echo, CT contrast effect, and SUV max) were selected for multivariable analysis. Based on the multivariable analysis, the internal echo and CT contrast effects were significantly associated with lymph node metastasis.

Pathological factors were examined in 57 patients who could be evaluated using a biopsy specimen and compared between the pN(+) and pN(−) groups. There were significant differences in the budding score and vascular invasion and nearly significant YK classification (Table 3). Only the budding score of the lymph node metastasis cases showed a normal distribution. The population budding score is shown in Figure 2. The cut-off value, AUC, sensitivity, and specificity were 2.88, 0.76, 75.0%, and 57.4%, respectively.

Table 3. Pathological factors related to lymph node metastasis. Logistic regression analysis for pathological factors predicting lymph node metastasis.

Pathological Factor		pN(+) Group	pN(−) Group	χ^2 Test *p* Value	Result of Logistic Regression Analysis					
					Univariate Analysis			Multivariable Analysis		
		n = 20	*n* = 37		OR	95% Cl	*p* Value	OR	95% Cl	*p* Value
Budding score		5.12 ± 3.57	2.24 ± 2.12	<0.001 **	1.44	1.17–1.87	<0.001 **	1.30	0.99–1.73	0.043 *
ly	none	20	37	-	-	-	-	-	-	-
	positive	0	0							
v	none	12	34	0.004 *	7.56	0.85–39.1	0.042 *	3.31	0.17–20.6	0.172
	positive	8	3							
pn	none	20	35	0.290	-	-	-	-	-	-
	positive	0	2							
YK classification										
	2/3	0/13	6/27	0.069	3.54	0.88–15.7	0.075	1.87	0.33–10.3	0.467
	4C/4D	4/2	3/1							

Budding score indicates average and standard deviation. ly: lymphatic vessel invasion, v: vascular invasion, pn: perineural invasion. YK classification: The borderline is slightly disordered in YK-2. The borderline is unclear, and large and small tumor nests are scattered in YK-3. The borderline is unclear, and small tumor nests invade in the form of a cord in YK-4C. The borderline is unclear, and the tumor does not form nests and diffusely invades in YK-4D. * $p< 0.05$, ** $p< 0.01$.

Based on χ^2 Test and univariate analysis of pathological factors, the budding score and vascular invasion were significantly associated with lymph node metastasis. As a result of the forward stepwise selection method, three factors (budding score, vascular invasion, and YK classification) were selected for multivariable analysis. The budding score was only significant in the multivariable analysis (*p*-value = 0.04, OR: 1.30, 95% CI: 0.99–1.73).

When the logistic regression analysis for predicting lymph node metastasis was performed using the factors budding score, vascular invasion, and YK classification, the following regression equation was derived:

Logit(*p*) = −1.89 + 0.26(budding score) + 1.19(vascular invasion: positive = 1, negative = 0) + 0.63(YK classification: 4C and 4D = 1, other = 0). If logit(0) $\geqq$ 0.5, then the patients have cervical lymph node metastasis.
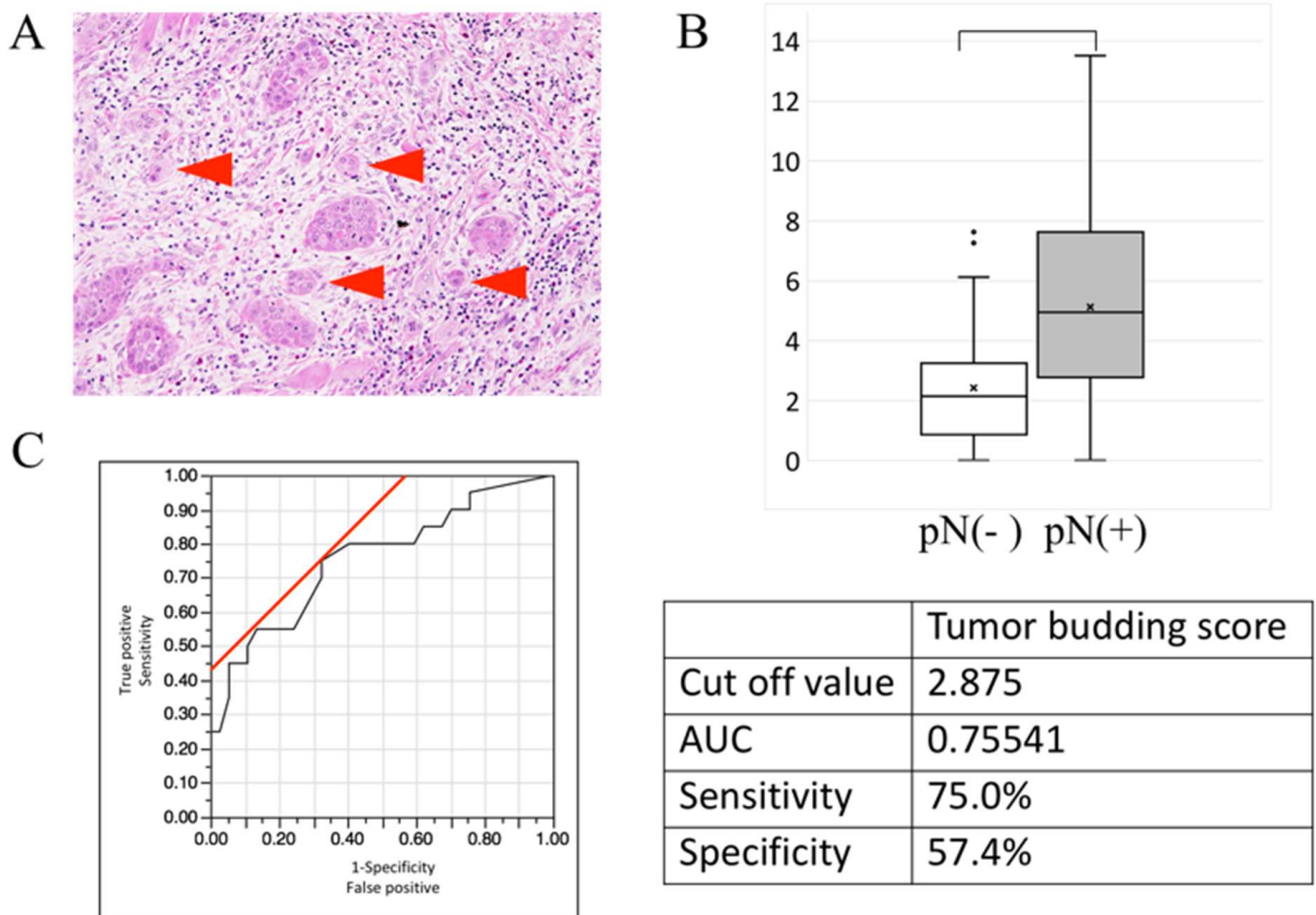
Figure 2. (**A**): Histopathological finding of tumor budding in biopsy specimen with hematoxylin and eosin (HE) staining of OSCC at 20 × 10 magnification. Red triangle indicate tumor buddings. (**B**): Tumor budding distribution of the tumor budding score. The central line is the median. mark "×" is average. The box is the 25–75% confidence interval. The vertical line is the 95% confidence interval. The dots are outliers. (**C**): ROC curve. Red line is tangent line with slope 1.

4. Discussion

Although various imaging systems are used to diagnose cervical lymph node metastasis in OSCC, the diagnosis of micro lesions in which the disease has not progressed is made comprehensively by a skilled diagnostician using various imaging systems, and this is thought to be the cause of the difference in diagnostic accuracy among institutions. Therefore, we started this study to create a diagnostic system that does not depend on a skilled diagnostician.

Recently, the NCCN guidelines indicated that margin positivity, perineural invasion, vascular invasion, and lymphatic invasion of the excision specimen were pathological risk factors for OSCC. However, these factors are not predictors of cervical lymph node metastasis. The aim of this study was to explore factors associated with cervical metastasis using preoperative imaging and histopathologic findings in order to diagnose cervical lymph node metastasis in OSCC. In this study, we identified imaging findings and pathologic factors associated with cervical lymph node metastasis and developed diagnostic criteria that combined these findings and suggested a treatment plan to improve the prognosis of oral squamous cell carcinoma.

4.1. Imaging Analysis

We focused on the imaging factors of CT, US, and FDG-PET. CT and US revealed the shape change in the cervical lymph node. In this study, the pN(+) lymph nodes had an average long diameter of 11.9 mm, a minor axis of 6.5 mm, and a long/short ratio of 2.2 mm, which were significantly different from the pN(−) lymph nodes. A previous study reported that metastatic lymph nodes have a 10 > mm long diameter, 5 > mm short diameter, and $2 \leqq$ long/short ratio [11]. US is able to visualize keratin formation due to micro metastasis foci as the presence of an internal echo and absence of a hilum, which has been reported to have high diagnostic accuracy [12,13]. In this study, the disappearance of the hilum and the appearance of internal echogenicity were significantly different between the pN(+) lymph nodes and pN(−) lymph nodes.

CT has a high accuracy in drawing anatomical positional relationships and largescale changes in the internal structure of metastatic lymph nodes using contrast agents, but it has less ability to draw small changes in lymph nodes than US.

The combined use of 18F-FDG PET with CT has enhanced the anatomic delineation and metabolic changes of cervical lymph node metastasis [14]. Previous studies have shown the superior sensitivity of 18F-FDG PET or PET/CT to CT/MR imaging for the detection of cervical lymph node metastasis in oral squamous cell patients [15–19].

We investigated the SUV max and the average of each cervical lymph node. The SUV max cut-off value for PET/CT in this study was 2.81, which is close to the value of 2.50 reported by Caylakl et al. [20]. In this study, we considered the possibility that micro metastases in the lymph node might affect the SUV of the lymph node and compared the SUV max and SUV average. The AUC of the SUV max was 0.804 and of the SUV average was 0.706, which means the SUV max was more useful than the SUV average. This finding suggests that the SUV max might reflect micro metastasis in cervical lymph nodes rather than the SUV average. Recently, quantifiable metabolic parameters such as the SUV peak, metabolic tumor volume (MTV), and total lesion glycolysis (TLG) obtained using 18F-FDG PET/CT have shown prognostic significance in several solid tumors and lymphomas in primary lesions [21,22]. These parameters need some lesion volume; therefore, they are difficult to apply to small lesions such as cervical lymph nodes but might be useful parameters to replace the SUV max if the spatial resolution of PET improves.

Based on the univariate analysis of imaging factors, there was a significant difference in the long diameter, short diameter, long/short ratio, internal echo, CT rim enhancement, SUV max, and SUV average, but based on the multivariable analysis, only the internal echo was observed. The appearance of rim enhancement and internal echoes are common findings that are considered diagnostic of cervical lymph node metastasis, and their association with metastasis was suggested in the multivariable analysis in this study. Other factors that showed significant differences only in the univariate analysis were considered informative factors, although they were not significant findings for predicting the diagnosis of metastasis.

4.2. Pathological Factor

In this study, we investigated the tumor budding score, lymphatic invasion, vascular invasion, nerve invasion, and YK classification. Tumor budding is defined as a cancer nest consisting of one or fewer than five component cells infiltrating into the stromal area of advanced cancer growth [8,23] and has recently been reported to correlate with metastasis and prognosis in oral cancer [24–27]. Many other studies report that the evaluation of resected specimens may be useful for predicting whether late metastasis may occur after initial treatment, but the purpose of this study is to investigate if these features could improve the accuracy of the diagnosis of lymph node metastasis before surgery. Therefore, we investigated the tumor budding score of the biopsy section. A significant difference was observed between the group with cervical lymph node metastasis and the group without metastasis. These results suggest that the budding score of biopsy sections may be useful for the diagnosis of metastasis before surgery. However, the cutoff value of 2.88 derived

from the ROC curve has a low specificity of 57.4%, and there is a possibility that nearly half of the unnecessary neck dissections may be performed for clinical application, so it should be used as a reference only.

Regarding the classification of tumor invasion, Matthias Troeltzsch et al., reported that G classification is correlated with recurrence and prognosis [28]. However, there is a report that the G classification has a low correlation with prognosis and that the diffuse infiltration pattern at the deep border is important [29]. In this study, we compared the YK classification. Although it has been reported that the YK classification correlates with cervical metastasis [30], it is a widely used index to predict the grade of oral cancer in Japan. In this study, the YK classification showed a significant difference in the presence of metastasis between the 1, 2, and 3 groups and the 4C and 4D groups using univariate analysis. The relationship between the presence of vascular invasion and lymph node metastasis has been reported in past studies [7,31]. In this study, the presence of vascular invasion showed a significant difference using the univariate analysis.

4.3. New Established Diagnostic Chart System

Based on the above result, we suggested a diagnostic chart system combining the imaging and pathological findings to diagnose lymph node metastasis (Figure 3). Rim enhancement with enhanced CT or the appearance of internal echoes with US are the most important diagnostic factors of metastasis. If there were no metastases, then PET SUV max ≥ 2.8 was defined as the border of metastasis in each lymph node. If the imaging findings did not indicate signs of lymph node metastasis, then the budding score and valvular invasion in the biopsy specimen were used as references for diagnosis.
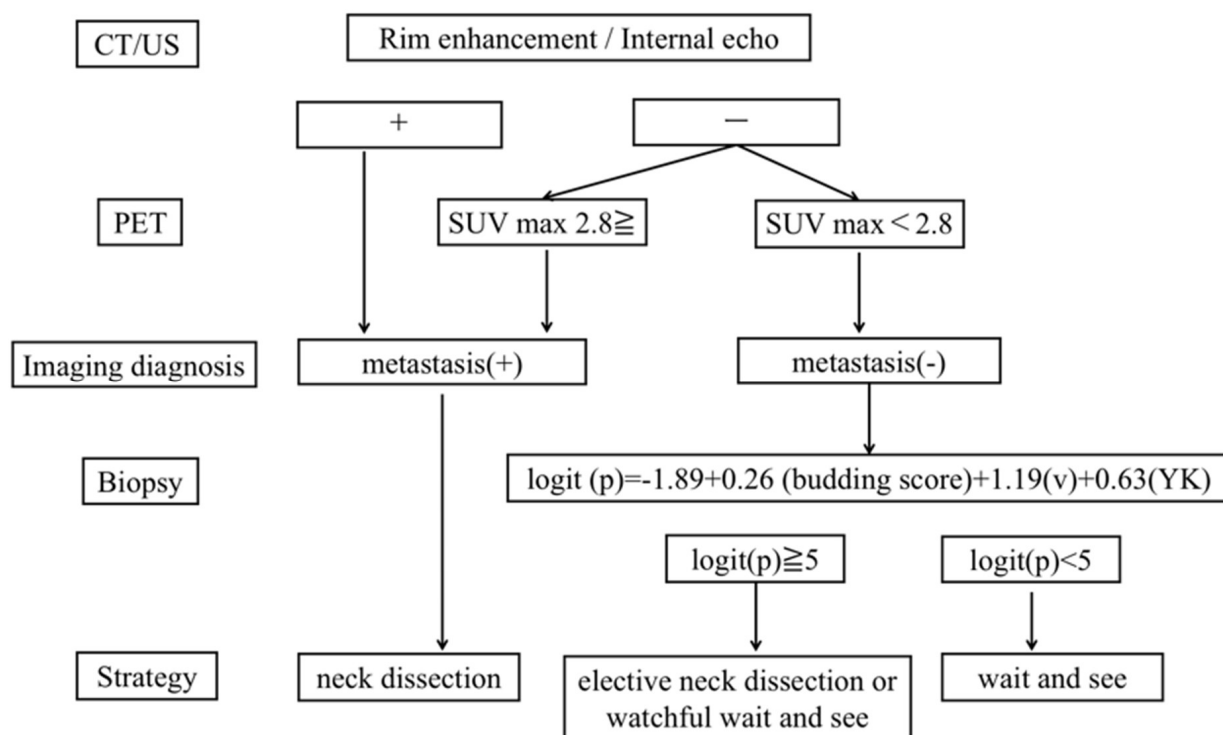

Figure 3. Diagnostic criteria and therapeutic strategy combining preoperative imaging and pathological findings for lymph node metastasis of oral squamous cell carcinoma.

If the logit(p) becomes ≥ 5, then the patient is considered to be at high risk for occult cervical metastasis, and either cervical lymphatic prophylactic neck dissection or careful follow-up should be considered.

Fifty-seven patients in this study adopted this diagnostic chart system; twenty-eight patients were only diagnosed as cN(+) using imaging, and fourteen of them were pN(+).

Twenty-nine patients were diagnosed with cN0 using imaging factors, but five patients had a high risk of cervical lymph node metastasis according to the biopsy specimen findings, and four of them had cervical lymph node metastasis. Twenty-two patients were diagnosed with cN0 using this chart system, but two patients had occult metastasis.

4.4. Limitations

In this study, late T2 and higher patients received preoperative radiation chemotherapy. Therefore, the possibility that the micro metastasis has disappeared cannot be ruled out, and it may have affected the pathological diagnosis of metastatic lymph nodes. In addition, 73 cases could be examined for imaging factors, and only 57 cases could be histopathologically examined. It is considered necessary to accumulate more cases.

The TNM classification was revised to 8th in 2017, and T was classified according to depth in invasion (DOI), and it is reported that the possibility of cervical lymph node metastasis is increased in patients with a DOI of 5→8. However, in this study, patients were diagnosed based on the 7th TNM classification, and patients with more than late T2 received neoadjuvant therapy; therefore, DOI could not be considered. In order to add DOI to this diagnostic system, DOI needs to be evaluated in patients without neoadjuvant therapy.

5. Conclusions

From this study, it was considered that the long diameter, short diameter, long/shot ratio, the SUV max imaging factor, the budding score, and YK classification of the biopsy specimen imaging factor were correlated with cervical lymph node metastasis.

In addition, the appearance of the internal echo of US, rim enhancement of the enhanced CT imaging factors, and the presence of vascular invasion in pathological factors were independent prognostic factors of cervical lymph node metastasis. We suggest that the diagnostic criteria and therapeutic strategy method of combining imaging factors and pathological factors might improve the diagnostic accuracy of cervical lymph node metastasis.

References

1. Beenken, S.W.; Krontiras, H.; Maddox, W.A.; Peters, G.E.; Soong, S.; Urist, M. T1 and T2 squamous cell carcinoma of the oral tongue: Prognostic factors and the role of elective lymph node dissection. *Head Neck* **1999**, *21*, 124–130. [CrossRef]
2. Okamoto, M.; Nishimine, M.; Kishi, M.; Kirita, T.; Sugimura, M.; Nakamura, M.; Konishi, N. Prediction of delayed neck metastasis in patients with stage I/II squamous cell carcinoma of the tongue. *J. Oral Pathol. Med.* **2002**, *31*, 227–233. [CrossRef] [PubMed]
3. El-Naaj, I.A.; Leiser, Y.; Shveis, M.; Sabo, E.; Peled, M. Incidence of Oral Cancer Occult Metastasis and Survival of T1-T2N0 OralCancer Patients. *J. Oral Maxillofac. Surg.* **2011**, *69*, 2674–2679. [CrossRef]

4. Tânia, A.; Addah, F.; André, C.; Clóvis, P.; Luiz, K. Predictive factors of occult metastasis and prognosis of clinical stages I and II squamous cell carcinoma of the tongue and floor of the mouth. *Oral Oncol.* **2004**, *40*, 780–786. [CrossRef]

5. Fernando, L.D.; Roberto, A.L.; Jacob, K.; Terence, P.F.; Jose, N.S.; Gabriel, M.; Geraldo, M.S. Relevance of Skip Metastases for Squamous Cell Carcinoma of the Oral Tongue and the Floor of the Mouth. *Otolaryngol. Head Neck Surg.* **2006**, *134*, 460–465. [CrossRef]

6. Ishida, T.; Hijioka, H.; Kume, K.; Yoshimura, T.; Miyawaki, A.; Nozoe, E.; Suenaga, S.; Indo, H.; Majima, H.; Nakamura, N. A diagnosis system for detecting cervical lymph node metastasis in oral squamous cell carcinoma: Collective consideration of the results of multiple imaging modalities. *J. Oral. Maxillofac. Surg. Med. Pathol.* **2017**, *29*, 210–216. [CrossRef]

7. Barnier, J.; Domenge, C.; Ozahin, M.; Matuszewska, K.; Lefèbvre, J.L.; Greiner, R.H.; Giralt, J.; Maingon, P.; Rolland, F.; Bolla, M.; et al. Postoperative Irradiation with or without Concomitant Chemotherapy for Locally Advanced Head and Neck Cancer. *N. Engl. J. Med.* **2004**, *350*, 1945–1952. [CrossRef]

8. Wang, C.; Huang, H.; Huang, Z.; Wang, A.; Chen, X.; Huang, L.; Zhou, X.; Liu, X. Tumor budding correlates with poor prognosis and epithelial-mesenchymal transition in tongue squamous cell carcinoma. *J. Oral Pathol. Med.* **2011**, *40*, 545–551. [CrossRef]

9. Xie, N.; Wang, C.; Liu, X.; Li, R.; Hou, J.; Chen, X.; Hung, H. Tumor budding correlates with occult cervical lymph node metastasis and poor prognosis in clinical early-stage tongue squamous cell carcinoma. *J. Oral Pathol. Med.* **2014**, *44*, 266–272. [CrossRef]

10. Sakata, J.; Yamana, K.; Yoshida, R.; Matsuoka, Y.; Kawahara, K.; Arita, H.; Nakashima, H.; Nagata, M.; Hirosue, A.; Kawaguchi, S.; et al. Tumor budding as a novel predictor of occult metastasis in cT2N0 tongue squamous cell carcinoma. *Hum. Pathol.* **2018**, *76*, 1–8. [CrossRef]

11. Steinkamp, H.; Cornehl, M.; Hosten, N.; Pegios, W.; Vogl, T.; Felix, R. Cervical lymphadenopathy: Ratio of long-to short-axis diameter as a predictor of malignancy. *Br. J. Radiol.* **1995**, *68*, 266–270. [CrossRef]

12. Yuasa, K.; Kawazu, T.; Nagata, T.; Kanda, S.; Ohishi, M.; Shirasuna, K. Computed tomography and ultrasonography of metastatic cervical lymph nodes in oral squamous cell carcinoma. *Dentomaxillofac. Radiol.* **2000**, *29*, 238–244. [CrossRef]

13. Norling, R.; Buron, B.; Therkilden, M.H.; Henriksen, B.M.; Buchwald, C.; Nielsen, M.B. Staging of Cervical Lymph Nodes in Oral Squamous Cell Carcinoma: Adding Ultrasound in Clinically Lymph Node Negative Patients May Improve Diagnostic Work-Up. *PLoS ONE* **2014**, *20*, e90360. [CrossRef]

14. Ceylan, Y.; Omur, O.; Hatipoglu, F. Contribution of (18)F-FDG PET/CT to staging of head and neck malignancies. *Mol. Imaging Radionucl. Ther.* **2018**, *27*, 19–24. [CrossRef]

15. Ng, H.; Yen, C.; Liao, T.; Chang, T.; Chan, C.; Ko, F.; Wang, M.; Wong, F. 18F-FDG PET and CT/MRI in oral cavity squamous cell carcinoma: A prospective study of 124 patients with histologic correlation. *J. Nucl. Med.* **2005**, *46*, 1136–1143.

16. Roh, J.L.; Yeo, N.K.; Kim, J.S.; Lee, J.H.; Cho, K.J.; Choi, S.H.; Nam, S.Y.; Kim, S.Y. Utility of 2-[18F] fluoro-2-deoxy-d-glucose positron emission tomography and positron emission tomography/computed tomography imaging in the preoperative staging of head and neck squamous cell carcinoma. *Oral Oncol.* **2007**, *43*, 887–893. [CrossRef]

17. Laimer, J.; Lauinger, A.; Steinmassl, O.; Offermanns, V.; Grams, A.; Zwlger, B.; Bruckmoser, E. Cervical lymph node metastasis in oral squamous cell carcinoma-How much imaging do we need? *Diagnostics* **2020**, *10*, 199. [CrossRef]

18. Bae, M.R.; Roh, J.L.; Kim, J.S.; Lee, J.H.; Cho, K.J.; Choi, S.H.; Nam, S.Y.; Kim, S.Y. 18F-FDG PET/CT versus CT/MR imaging for detection of neck lymph node metastasis in palpably node-negative oral cavity cancer. *J. Cancer Res. Clin. Oncol.* **2020**, *46*, 237–244. [CrossRef]

19. Linz, C.; Brands, C.R.; Herterich, T.; Hartmann, S.; Richter, M.U.; Kubler, C.A.; Hang, L.; Kertels, O.; Bley, A.T.; Dierks, A.; et al. Accuracy of 18-F Fluorodeoxyglucose Positron Emission Tomographic/Computed Tomographic Imaging in Primary Staging of Squamous Cell Carcinoma of the Oral Cavity. *JAMA Open* **2021**, *4*, e217083. [CrossRef]

20. Caylakli, F.; Yilmaz, S.; Ozer, C.; Reyhan, M. The Role of PET-CT in Evaluation of Cervical Lymph Node Metastases in Oral Cavity Squamous Cell Carcinomas. *Turk. Arch. Otorhinolaryngol.* **2015**, *53*, 67–72. [CrossRef]

21. Cheng, G.; Huang, H. Prognostic value of 18F-fluorodeoxyglucose PET/computed tomography in non–small-cell lung Cancer. *PET Clin.* **2018**, *13*, 59–72. [CrossRef] [PubMed]

22. Albano, D.; Bosio, G.; Bianchetti NPagani, C.; Re, A.; Tucci, A.; Giubbini, R.; Bertagna, F. Prognosticroleofbaseline18F-FDG PET/CT metabolic parameters in mantle cell lymphoma. *Ann. Nucl. Med.* **2019**, *33*, 449–458. [CrossRef] [PubMed]

23. Lai, W.; David, K.; Hugh, M.; Jacintha, O.; David, F.; John, H.; Diarmuid, O.; Kieran, S. Tumor budding is a strong and reproducible prognostic marker in T3N0 colorectal cancer. *Am. J. Surg. Pathol.* **2009**, *33*, 134–141. [CrossRef]

24. Helvécio, J.; Priscila, L.R.L.; Victória, M.; Ângela, C.; Paulo, S.; Maria, A.; Martinho, H. Cell proliferation is associated with intensity of tumor budding in oral squamous cell carcinoma. *J. Oral Pathol. Med.* **2018**, *47*, 128–135. [CrossRef]

25. Yamada, S.; Otsuru, M.; Yanamoto, S.; Hasegawa, T.; Aizawa, H.; Kamata, T.; Yamakawa, N.; Kohgom, T.; Ito, A.; Noda, Y.; et al. Progression level of extracapsular spread and tumor budding for cervical lymph node metastasis of OSCC. *Clin. Oral Investig.* **2018**, *22*, 1311–1318. [CrossRef]

26. Yamakawa, N.; Kirita, T.; Umeda, M.; Yanamoto, S.; Ota, Y.; Otsuru, M.; Okura, M.; Kurita, H.; Yamada, S.; Hasegawa, T.; et al. Tumor budding and adjacent tissue at the invasive front correlate with delayed neck metastasis in clinical early-stage tongue squamous cell carcinoma. *J. Surg. Oncol.* **2019**, *119*, 370–378. [CrossRef]

27. Mscitti, M.; Tongi, L.; Caponio, V.; Zhurakivska, L.; Muzio, L.; Rubini, C.; Santnrelli, A.; Triano, G. Prognostic significance of tumor budding thresholds in oral tongue squamous cell carcinoma. *Oral Dis.* **2022**. [CrossRef]

28. Matthias, T.; Selgai, H.; Sophie, B.; Markus, T.; Florian PMichael, E.; Sven, O. What Factors Are Associated with Regional Recurrence After Operative Treatment of Oral Squamous Cell Carcinoma? *J. Oral Maxillofac. Surg.* **2018**, *76*, 2650–2659. [CrossRef]

29.   Barnes, L.; Eveson, J.; Reichart, P.; Sidransky, D. *World Health Organization Classification of Timours, Pathology & Genetics, Head and Neck Tumors*, 4th ed.; IARC Press: London, UK, 2005; pp. 168–175.

30.   Yamamoto, E.; Miyakawa, A.; Kohama, G. Mode of invasion and lymph node metastasis in squamous cell carcinoma of the oral cavity. *Head Neck Surg.* **1984**, *6*, 938–947. [CrossRef]

31.   Coper, J.S.; Pajak, T.F.; Forastiere, A.A.; Jacobs, J.J.; Campbell, B.H.; Saxman, S.B.; Kish, J.K.; Kim, H.E.; Cmelak, A.J.; Rotman, M.; et al. Postoperative concurrent radiotherapy and chemotherapy for high-risk squamous-cell carcinoma of the head and neck. *N. Engl. J. Med.* **2004**, *350*, 1937–1944. [CrossRef]